

## Article

# Factors Affecting the Rates and Modes of Landslide Colluvium Removal in River Channels of Podhale (Western Carpathians)

Józef Kukulak <sup>1,\*</sup>, Karol Augustowski <sup>1,\*</sup>  and Janusz Olszak <sup>2</sup> <sup>1</sup> Pedagogical University of Kraków, Institute of Geography, Podchorążych 2, 30-084 Kraków, Poland<sup>2</sup> AGH University of Science and Technology, Faculty of Geology, Geophysics and Environmental Protection, Mickiewicza 30, 30-059 Kraków, Poland

\* Correspondence: karol.augustowski@up.krakow.pl; Tel.: +48-692-193-931

**Abstract:** This paper presented some hydrological factors affecting the course and rate of fluvial erosion of landslide colluvium at its contact with river flow. Volumes of colluvium eroded by rivers in the period 2013–2019 were measured at Podhale (a part of Polish West Carpathians) on four landslides representing various geological settings. At each landslide, changes in shape and position of the contact zone between colluvium and river water were registered after episodes of high river stage. The obtained data on changes in relief of the landslide fronts and adjacent river channels were used to calculate volumes of colluvium removed during each episode. The course of erosion and volumes of colluvium eroded were compared with the water stage records for the studied period of time. Intensity of colluvium erosion was found to be strongly dependent on the water levels and cohesion of colluvium. Volumes of removed colluvium were the greatest during short-lived (1–2 days) and prolonged (7–10 days) periods of high river stages. The rate of erosional removal was the highest for colluvium consisting of poorly consolidated Quaternary matrix-supported massive gravel and overlying fine deposits stored within river terraces. Colluvium composed of Neogene mudstones and sandstones was removed at a lower rate and the rate of removal was lowest for large blocks and slices composed of solid layers of alternating sandstone and shales belonging to the Podhale Flysch series. Erosion of the landslide toes was more intense at those sites where the river flow approached the landslide front at a wider angle.

**Keywords:** landslides; river channels; fluvial erosion; Polish West Carpathians

**Citation:** Kukulak, J.; Augustowski, K.; Olszak, J. Factors Affecting the Rates and Modes of Landslide Colluvium Removal in River Channels of Podhale (Western Carpathians). *Water* **2022**, *14*, 3577. <https://doi.org/10.3390/w14213577>

Academic Editor: Ian Prosser

Received: 9 October 2022

Accepted: 4 November 2022

Published: 7 November 2022

**Publisher's Note:** MDPI stays neutral with regard to jurisdictional claims in published maps and institutional affiliations.



**Copyright:** © 2022 by the authors. Licensee MDPI, Basel, Switzerland. This article is an open access article distributed under the terms and conditions of the Creative Commons Attribution (CC BY) license (<https://creativecommons.org/licenses/by/4.0/>).

## 1. Introduction

Tongues of many landslides descending from valley slopes, and most of those descending from river banks, reach river channels. Encroachment of colluvial masses usually disturbs the hydraulic regime of rivers [1–4]. A new source of debris, abundant in some cases, appears in places where no such supply was present before. Depending on the nature and volume of debris, rivers adjust their capacity to remove the debris downstream from the landslide toes. When the volume of colluvium is large and blocks the river flow, a dam lake with aggrading sediments may form in the impounded part of a valley floor [5–12]. On broad enough valley floors river channels may shift away from landslide fronts or be avulsed [11,13–20]. Variants of river adjustment to the encroachment of colluvium into river channels are described from New Zealand [18], Himalaya and India [8,12,21,22], and North America [23], among others. In Poland, examples are provided by landslides in the Carpathians [5,24–29], the Sudetes [3], and on the steep banks of the Vistula river [30,31].

Most studies upon the relation between rivers and landslides focus on the lateral erosion by the rivers causing landslides on river banks or reactivating earlier landslides during floods, which are considered as the main trigger [32–35]. The farther stage of this interaction—the mode and rate of colluvium removal from the river channel—remains less studied. However, this is the stage when river channels are being reshaped and landslides

respond to the fluvial erosion. This perpetual interaction between erosion, colluvium removal by rivers, and the unsteady movement of landslide results in the position of the colluvium–river contact zone (C-RCZ) changing at various rates and directions. No published detailed studies are available on the dynamics of such contact zones, especially for colluvium of variable lithology, for multiyear periods and with data on changing river stages available for comparison. Most studies concentrate on the results of rapid incursion of colluvial masses into river channels [17,18,36–40] and on the reactivation of landslides in relation to their shearing resistance and the degree of their consolidation [41–44].

This study presented a description and interpretation of the evolution of four C-RCZs differing between them in type and lithology of colluvium, landslide tongue mobility, shape and size of river channels, and in the temporal dynamics of river discharge. Keeping in mind the variety of factors contributing to the dynamics of such contact zones (e.g., intensity of precipitation, rate of water infiltration into colluvium, mechanical properties of colluvium, potential mobility landslide tongues, structure of river channels), we concentrated largely on the hydrological factor. Large oscillations of river stages obviously stimulate fluvial erosion of colluvium in river channels. The rates and volumes of erosion of those landslide parts (toes) which became available for fluvial processes were studied.

We used data from multiyear monitoring of the fluvial erosion of colluvium to find (i) to what degree of the rising river stages correlate with the phases of increased erosion of colluvium in the C-RCZs and (ii) to what degree of other factors may contribute to differences in erosion rates between the studied sites. Another aim of our study was to find whether the greatest loss of colluvium takes place during short-lived (1–2 days) episodes of maximum water stages or during prolonged (7–10 days) periods of high river stage. We also investigated the effectiveness of fluvial erosion relative to the seasonal distribution of water-stage oscillations.

## 2. Study Area

The studied landslides are located in the Central Western Carpathians and adjacent part of the Outer Western Carpathians, at the foothills of the Tatra Mountains. That part of Podhale includes a fragment of the Gubałowskie Foothills (1025 m), underlain by Podhale Flysch series, and its boundaries are the Pieniny Klippen Belt (773 m) and Orava Basin (600 m). The latter one is a tectonic basin filled up with Neogene freshwater mudstones, claystones, and sandstones and overlying Quaternary alluvial sediments. Our investigation sites were situated at four landslide toes invading the channels of the Czarny Dunajec River (site 1—Chochółów) and its three tributaries: Wielki Rogoźnik (site 2—Ludźmierz), Bystry (site 3—Czerwona Góra), and Cichy (site 4—Grapa) (Figure 1). Two of the landslides (sites 1 and 2) have already been the subject of investigations concerning their origin and relief transformation [45]. However, the landslide degradation and river erosion of their toes were not accounted for.

Hydrological regimes of the rivers responsible for the landslide erosion are controlled by atmospheric precipitation. The average annual precipitation in this region is about 900–1100 mm, with ca. 700 mm in dry years and ca. 1250 mm in wet years. The precipitation is the highest during the summer months with about 130 mm in June and July when torrential rains prevail [46]. The daily precipitation often exceeds 40 mm, occasionally even 100 mm [47–49]. Steep slopes in the area favor rapid drainage to the river channels where floods are accompanied by intense morphodynamic processes in river channels. Winter precipitation is lower, largely retained in snow cover.

Air and ground temperatures fall below 0 °C during the winter semester. Common are oscillations of daily temperatures around 0 °C [48,50], resulting in multigelation—cyclical freezing and thawing of the ground surface, a factor important for erosion on river banks [51]. Snow cover lasts usually for 100–110 days a year and ice cover on the rivers lasts usually for 70–100 days. The two last mentioned values display large fluctuations in the recent years and the snow cover or river ice happen to disappear temporarily during the winters.

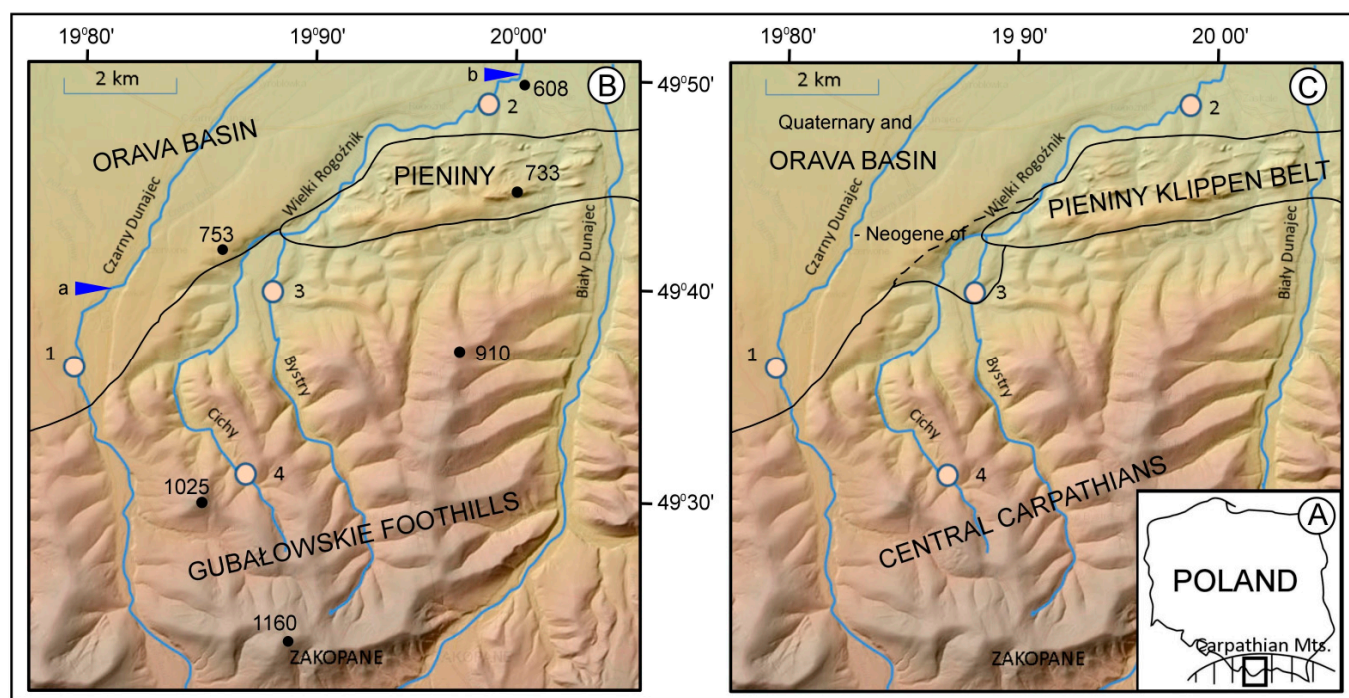


**Figure 1.** Location of the study sites in the Carpathians (A) and in morphology (B) and geology (C) Podhale. Study site: 1—Chocholów, 2—Ludźmierz, 3—Czerwona Góra, 4—Grapa. Water gauges: a—Koniówka, b—Ludźmierz, black dots—m a.s.l.

### 3. Methods

The course and rate of colluvium removal by the rivers at the study sites were investigated in the years 2013–2019. Detailed profiles of the undercut landslide fronts were measured and changes of the landslide-channel boundaries were repeatedly registered. Our field work included detailed geomorphological mapping of all landslides, especially their C-RCZs in the scale of 1:500. The C-RCZs were mapped 18 times during the study, of which 6 were times after spring thawing episodes (2013–2019) and 12 times after major water-level rises (2 times in 2013, 2015, and 2017, and 6 times in 2019). Each of the time locations of lateral river erosion of landslide toes were registered in the field and then the colluvium volume loss was estimated. The locations of colluvium loss were always clearly distinguished. Before each estimation, the volume of colluvium removal at every location of the C-RCZs was measured. The measurements were determined using a laser distance meter from two (sites 1, 2 and 3) and three (site 4) base-fixed points located on the opposite bank of the river channels. The distance from the base points to the C-RCZs was always measured according to the same azimuths (in every five degrees from the starting value). Photographic documentation was also used for identification of erosion occurrence and colluvium relief modifications at the C-RCZs. The height of the undercut landslide front was measured and the volume of colluvium removed was estimated after each water-level rise. Disturbances in relief of the landslide tongues indicative of their movement were registered. For that purpose, a terrestrial LiDAR imaging was used for site 1 that was obtained once at the beginning of our investigations. Daily recordings of water levels on the studied rivers in years 2013–2019 at the Ludźmierz and Koniówka gauging stations were taken from the IMGW's internet site ([www.hydro.imgw.pl](http://www.hydro.imgw.pl), accessed on 11 October 2020). The structure and texture of colluvium were determined in open fractures and at eroded frontal scarps on the tongues.

#### *Hydrological Conditions of the Studied C-RCZs in Years 2013–2019*

The studied C-RCZs differ in river channel structures and hydrological parameters of the rivers (Table 1). The river channels at the study sites are cut into gravelly deposits that

form a thin layer over the firm substrate of mudstones and clays (sites 1, 2 and 3) or flysch strata (site 4). The longitudinal profiles of the channels over the studied sections are rough, with pools and riffles (1, 2 and 3). At site 4, rocky steps are present in the channel formed on thick sandstone beds more resistant to erosion. Gradients of the channels in the C-RCZs vary between 3.0‰ and 32.1‰ (Table 1). Channel patterns are sinuous with wandering main flow (sites 1, 2 and 3) or nearly straight (site 4).

**Table 1.** Morphological and hydrological parameters of the rivers in studied C-RCZs.

Study Sites (1–4)	Elevation of Channel Floor (m a.s.l.)	Channel Gradient (‰)	Maximum Water Level (cm)	Mean Annual Discharge (m <sup>3</sup> /s)	Channel Width (m)	Position of Flow Relative to Landslide Front
Czarny Dunajec (1)	739–737	12.5	2.15	4.38	40–60	diagonal
Wlk. Rogoźnik (2)	602.5–600	3.0	1.55	2.0	8–12	transverse/diagonal
Bystry (3)	666–663	11.0	1.35	1.1 *	7–10	transverse
Cichy (4)	788–770	32.1	1.30	0.5 *	5–8	parallel

\*—estimated using IMGW data from the Ludźmierz gauging station.

The Czarny Dunajec and Wielki Rogoźnik rivers are similar in terms of the areas of their uppermost drainage basins. The former one has area of 134 km<sup>2</sup> till the Koniówka water gauge, and the latter one has area of 125 km<sup>2</sup> until the point of Ludźmierz water gauge [52]. From the other hand, environmental conditions make them different. The Czarny Dunajec River (1) displays the greatest discharges and the most equalized river stages over the course of the year because its waters come from the western part of the Tatra Mountains where values of rainfall and snowfall are high. The Wielki Rogoźnik River (2), whose upper courses are represented by the Bystry (3) and Cichy (4) rivers, drains only the foothills area of the Tatra (Gubałowskie Foothills), and hence the water stages and discharges are highly variable (Table 1). The uppermost catchment of the Czarny Dunajec River is located in the Tatra Mountains (57%), and that part of the basin is built of crystalline and carbonate rocks and is characterized by climate and vegetation altitudinal zonation (precipitation of 1800–1300 mm/yr) and a dense forestation of lower altitudinal zones [53,54]. However, the lower part of the basin is located within the Podhale region that features flysch series as the substrate, low-mountain relief, and the area occupied largely by agriculture. The Wielki Rogoźnik River basin is located exclusively within the low-mountain area. It is built of flysch series and insignificantly of flysch and carbonate strata in the zone of the Pieniny Klippen Belt. The basin is highly deforested and used as an agriculture area. The hydrological regime of both rivers is nival–pluvial at the foreland of the Tatra Mountains; however, the Czarny Dunajec River regime in the Tatras can be described as pluvio–nival [55].

The mean annual flow of the Czarny Dunajec at the Koniówka gauging station during the period 2013–2019 was 4.30 m<sup>3</sup>/s, while the maximum recorded value exceeded 200 m<sup>3</sup>/s (data from IMGW Kraków—[www.hydro.imgw.pl](http://www.hydro.imgw.pl), accessed on 11 October 2020). The mean annual flow at the gauging station Ludźmierz on the Wielki Rogoźnik was 2 m<sup>3</sup>/s, and maximum also exceeded 200 m<sup>3</sup>/s. The maximum values of flow were recorded in summer. April and May were marked by more frequent episodes of elevated water level, corresponding to snowmelt in the Tatra Mountains.

The river stages oscillated in the successive years of the study period. The mean annual flow in the Czarny Dunajec remained at ca. 150–170 cm, but the maximum flows exceeded 250 cm several times each year, while maximum daily flows attained up to 297 cm (19 July 2018). Stages above 200 cm were recorded 29 times during the study—six days uninterrupted in May 2014 and four days in July 2018 (Figure 2).

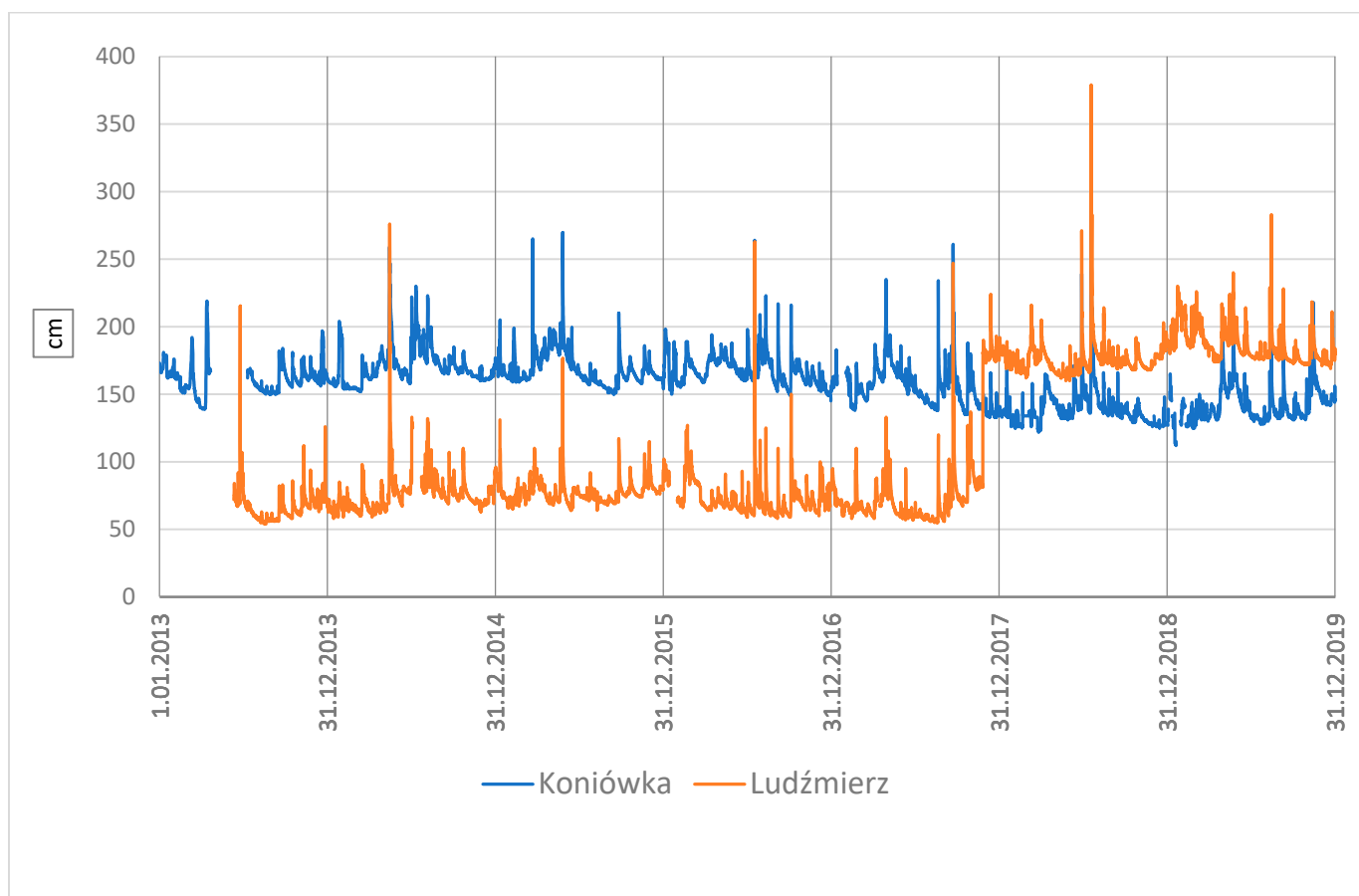


**Figure 2.** Oscillations of maximum daily water levels in the Czarny Dunajec River (Koniówka gauging station) and the Wielki Rogoźnik River (Ludźmierz gauging station; since 2017 the values are higher by 100 cm because of datum relocation).

Water level oscillations in the Wielki Rogoźnik River were much greater than in the Czarny Dunajec River. The mean water level was within the range of 60–70 cm, while the maximum values exceeded 100 cm several times each year, with values as high as 276 cm (16 May 2014), 263 cm (17 July 2016), 279 cm (19 July 2018) 283 cm (14 August 2019). The high water levels usually persisted for 2–3 days, during prolonged rainfalls even for six days (May 2014, July 2018). An extremely long high water stage persisted on the Wielki Rogoźnik—21 days above 100 cm—at the break of January and February 2019.

## 4. Results

### 4.1. The Landslides

Site 1 (Chochołów) is situated on the front of a rotational landslide 15 m long, 50 m wide, and ca. 800 m<sup>2</sup> in surface area. It has displaced alluvial matrix-supported massive gravel dating from MIS 3 and overlying fine deposits stored within a strath terrace [56]. Its detachment surface cuts also through the underlying non-stratified Neogene clayey mudstones. The gravel is composed mainly of granites and quartzites from the Tatra Mountains. Inclination of the landslide surface changes from nearly vertical at the main scarp to 10–15° in its lower part (Figure 3A). The front of colluvium descends to the river channel and is being undercut by lateral erosion. The landslide originated in 1980, and the greatest displacements took place in 1997 and 2001. A part of its head is still active and remodeling of its relief occurs in summer semesters which are the rainy seasons, and also during winter semesters—by multigelation [51]. The channel of the Czarny Dunajec is there over 80 m wide, with a gently sinuous course. The channel floor is paved with gravel shaped into numerous ephemeral erosional troughs and extensive lateral bars. The main flow and

lateral branches often change their positions during high discharge events, forming new gravel bars or modifying the existing ones (Figure 3B). One of the gravel bars now shields the front of colluvium that was being eroded until 2018. From a morphodynamic point of view, the river channel in this section is an erosional–redepositional one [57].

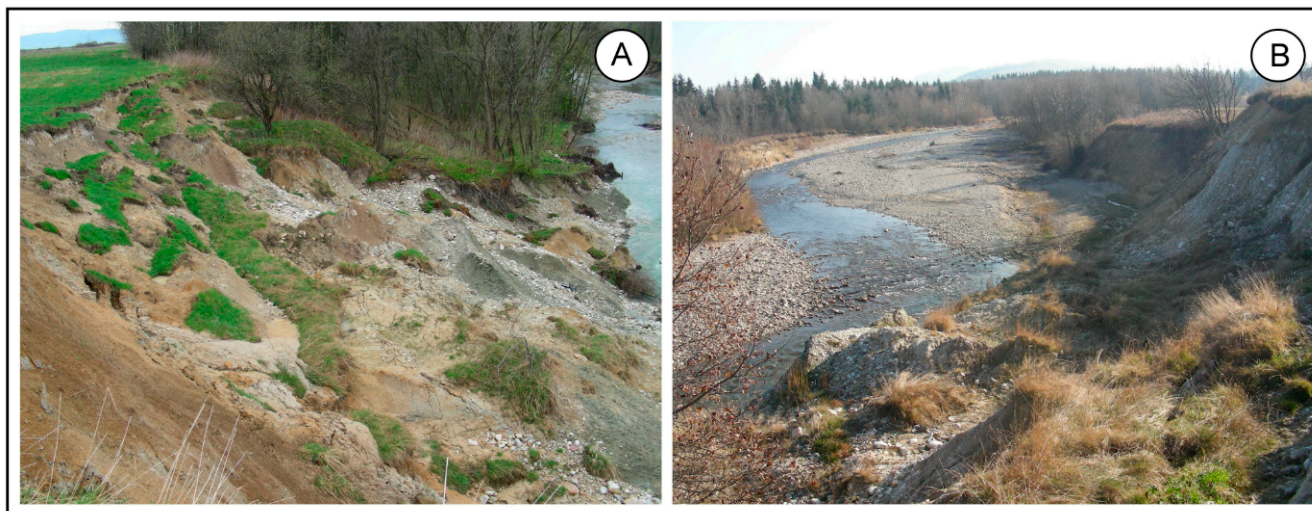


**Figure 3.** Chochółów landslide (site 1) being undercut by the Czarny Dunajec River; (A)—landslide relief; (B)—location of the Czarny Dunajec River channel in reference to the landslide toe.

At site 2 the Wielki Rogoźnik River erodes colluvium, which is also matrix-supported, and massive gravel and clays at the top slid off a 6–7 m high river terrace. The gravel is composed of highly weathered crystalline rocks and comes from a series 5–5.5 m thick, covered by silts 1.0–1.5 m thick, also present in colluvium (Figure 4A). They slid down toward the river channel over the surface of Neogene claystones, exposed in the channel bottom. The landslide was triggered by undercutting of a concave bank of a migrating river bend over its whole length (Figure 4B). The slid-down stripe of the bank is 17–30 m wide. The landslide has probably been active since 1934, but later floods extended it downstream, especially in 1997. Currently, the front of this landslide is stable, and no longer moves towards the river bed. Curvature of the bend is greatest in this extended NE part of the landslide and the C-R CZ evolves rapidly. During high river stages, that is, higher than 1.5 m, the part of colluvium adjacent to the channel is flooded and thus undergoes erosion. Erosion of colluvium in the SW part of the landslide is facilitated by its high degree of soaking with water that seeps from the adjacent peat bog. Prolonged action of these acid waters accelerates weathering of crystalline clasts in the gravel, which decompose to granular clay and become more susceptible to downslope creep toward the river channel.

Site 3 (Czerwona Góra) lies at the front of the youngest landslide on the right bank of the Bystry River. This landslide is a part of a series of landslides along the edge of the western slope of the Czerwona Góra Hill (696 m). Activation of landslides migrates slowly upstream and the youngest landslides, including that selected for site 3, are situated near the southern end of the hill. The landslide extends over the whole length of the slope. Its main scarp lies 20–23 m above the current river level (Figure 5A). It is a composite, rotational slide with three major phases of movement recognizable in its relief. The sediment that underwent sliding comes from a series of clayey mudstones and sands interlayered with gravel [58]. The section exposed in the main scarp consists mainly of distinctly stratified mudstone-sand packages (75%). The layers are thicker, up to 2 m, in the lower part of the section and are only 0.2–0.5 m thick in the middle and upper part. All sediments are firmly compacted. The attitude of the strata is  $75^\circ/25^\circ/\text{NW}$  and the azimuth of the river flow is  $15^\circ$ . The river approaches the front of colluvium at a right angle and then turns left to flow alongside the margin of colluvium. During high river stages, flow at this section often bifurcates as a result of proximal deposition of freshly eroded colluvium and alluvial gravel.

The detachment surface of the landslide is steep, nearly  $70^\circ$ , while displaced and internally disturbed colluvium is being deposited directly at the base of slope, filling a part the Bystry River channel. The frontal pile of colluvium was initially 1.2–1.6 m high and it occupied  $\frac{3}{4}$  of the earlier active channel width. During the successive water level rises, the front of colluvium was eroded and immediately restored with new supplies of colluvium from the reactivated landslide (Figure 5B). The landslide,  $1340 \text{ m}^2$  in area, originated in May 2014, but its lateral extension on the southern side was created in June 2018 and reactivated in May 2019.

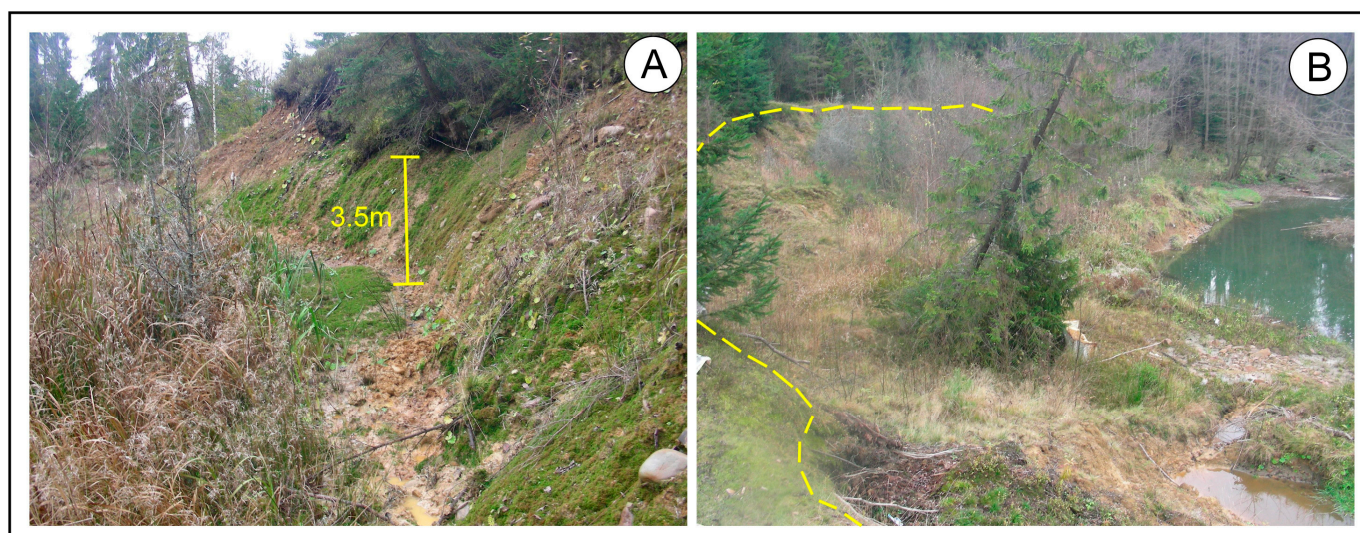


**Figure 4.** Ludźmierz landslide (site 2) being undercut by the Wielki Rogoźnik: (A)—gravel in the escarpment of the landslide, (B)—landslide surface.

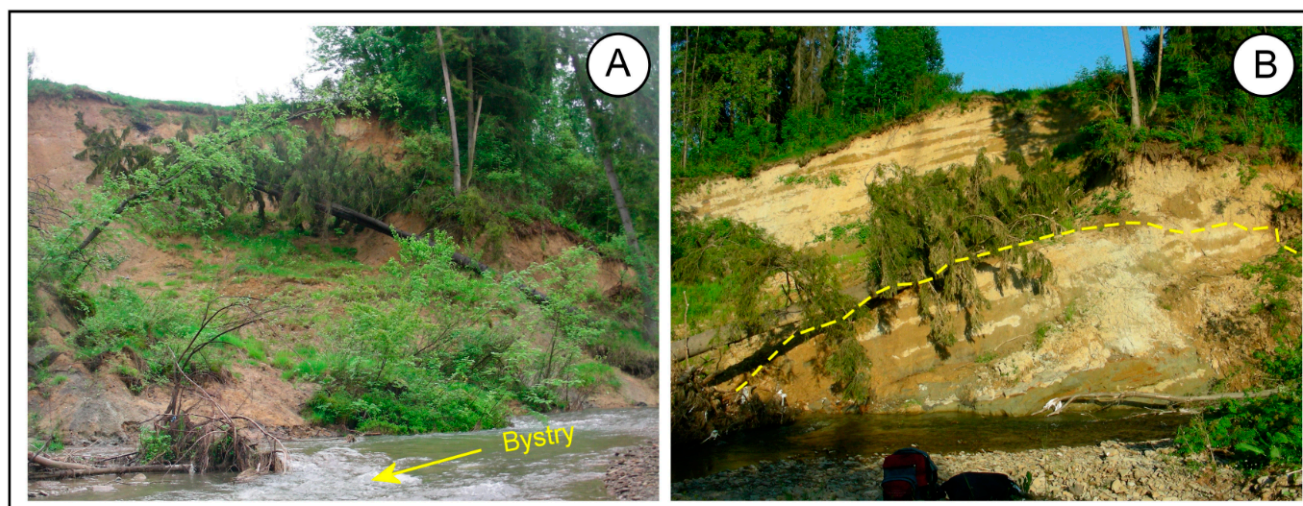


**Figure 5.** Czerwona Góra landslide (site 3) being undercut by the Bystry, (A)—Landslide tongue in 2015, (B)—eroded colluvium in the rejuvenated part of the landslide in 2017.

The landslide at site 4 (Grapa) is over  $1 \text{ km}^2$  in area and it is a deep structural consequent slide of a flysh series [59]. Its front is formed as a ridge of piled up colluvium, up to 15 m high and extending diagonally on the valley slope (Figure 6A). In the SW part of the landslide, the ridge enters the channel of the Cichy River and dams its flow. Prolonged dissection of the colluvial dam by fluvial erosion and removal of the sandstone and shale debris resulted in cutting a 12–15 m deep ravine along the front of the landslide tongue. The section of the ridge that is being eroded now is over 400 m long (Figure 6B). For some

100 m of its upstream section it does not dissect the whole thickness of colluvium. Farther downstream, the floor is composed of solid bedrock, with projecting edges of sandstone layers. As the course of the river follows the attitude of the layers and the layers dip under the bank opposite to the landslide, the south-west, right bank is being undercut more intensely than the front of the landslide tongue.

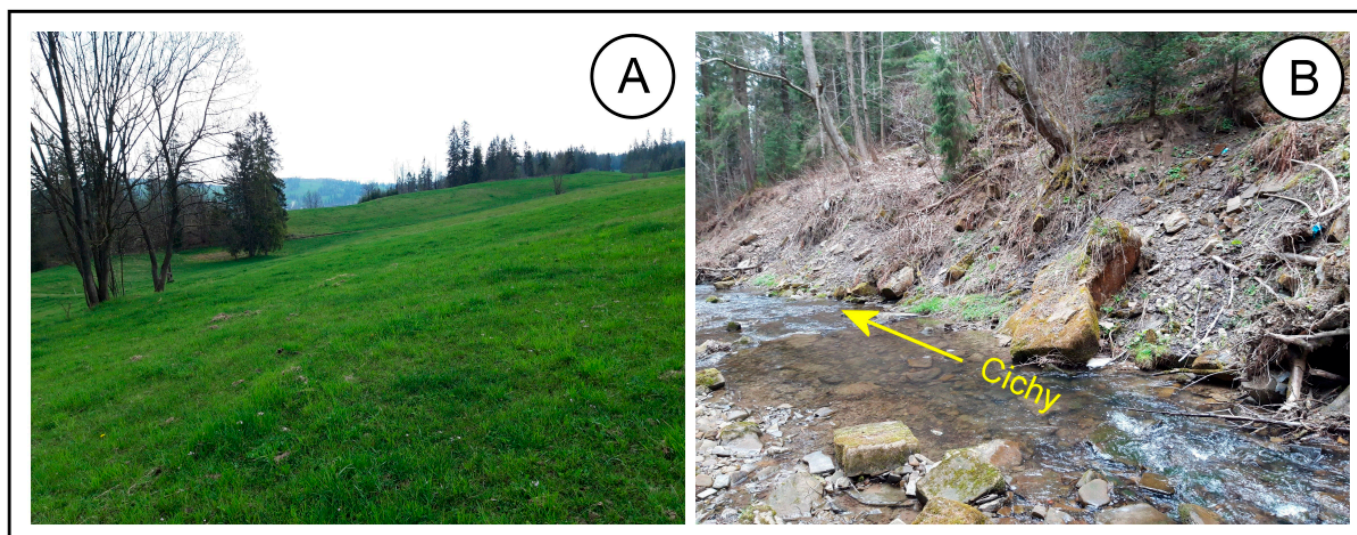


**Figure 6.** Grapa landslide (site 4); (A)—colluvial ridges on the valley slope, (B)—colluvial blocks in the channel of the Cichy River.

#### 4.2. The Course and Amounts of Colluvium Erosion at the Study Sites in Years 2013–2019

The total volume of colluvium removed by fluvial erosion from the C-RCZs in years 2013–2019 amounted to just over 360 m<sup>3</sup>. The values differed between the individual sites (Table 2) and the successive years. Episodes of increased erosion correspond to high river stages. The extent of fluvial erosion at the C-RCZs depended not only on the water level rises and their frequency. Other hydrological factors involved could be the erosional power of the rivers and sediment load [1,60,61]. The sites differed in geometries of the fluvial channels (Table 1) and in susceptibility of colluvium to erosion.

**Table 2.** Volumes of colluvium removed from the studies landslides in the period 2013–2019.

Site	Volume of Colluvium Removed from the Landslide Fronts (m <sup>3</sup> )							Total
	2013	2014	2015	2016	2017	2018	2019	
Chochołów (1)	15	26	18	19	21	14	17	130
Ludźmierz (2)	4	8	4	4	7	7	9	43
Czerwona Góra (3)	-	33	14	15	25	33	27	147
Ciche (4)	4	7	4	5	8	6	7	41
Total (1 + 4)	33	74	40	43	61	60	60	361

The total volume of rock eroded from site 1 during the seven years was evaluated at 130 m<sup>3</sup>. This includes colluvium consisting of gravel and silt slid down together with a detached top part of underlying Neogene clayey mudstones as well as stable underlying exposures of these mudstones (Figure 7C). The basal detachment of the landslide is a dispersed zone of discontinuities situated at the approximated depth to which the mudstones become soaked with groundwater infiltrating from the overlying gravel. The uneven zone of detachment is exposed in the river bank about 1 m above the water level (Figure 8A,B). During every high stage of the river, the Czarny Dunajec erodes the massive

cohesive mudstones of the undisturbed bedrock strata as well as the displaced and rotated colluvium above the detachment zone (Figure 7A,B). It may be estimated that about the third part of the 130 m<sup>3</sup> of eroded lithic material are the mudstones from beneath the landslide. The more prone to degradation colluvium was eroded at much faster rate than the underlying firm clayey mudstones.

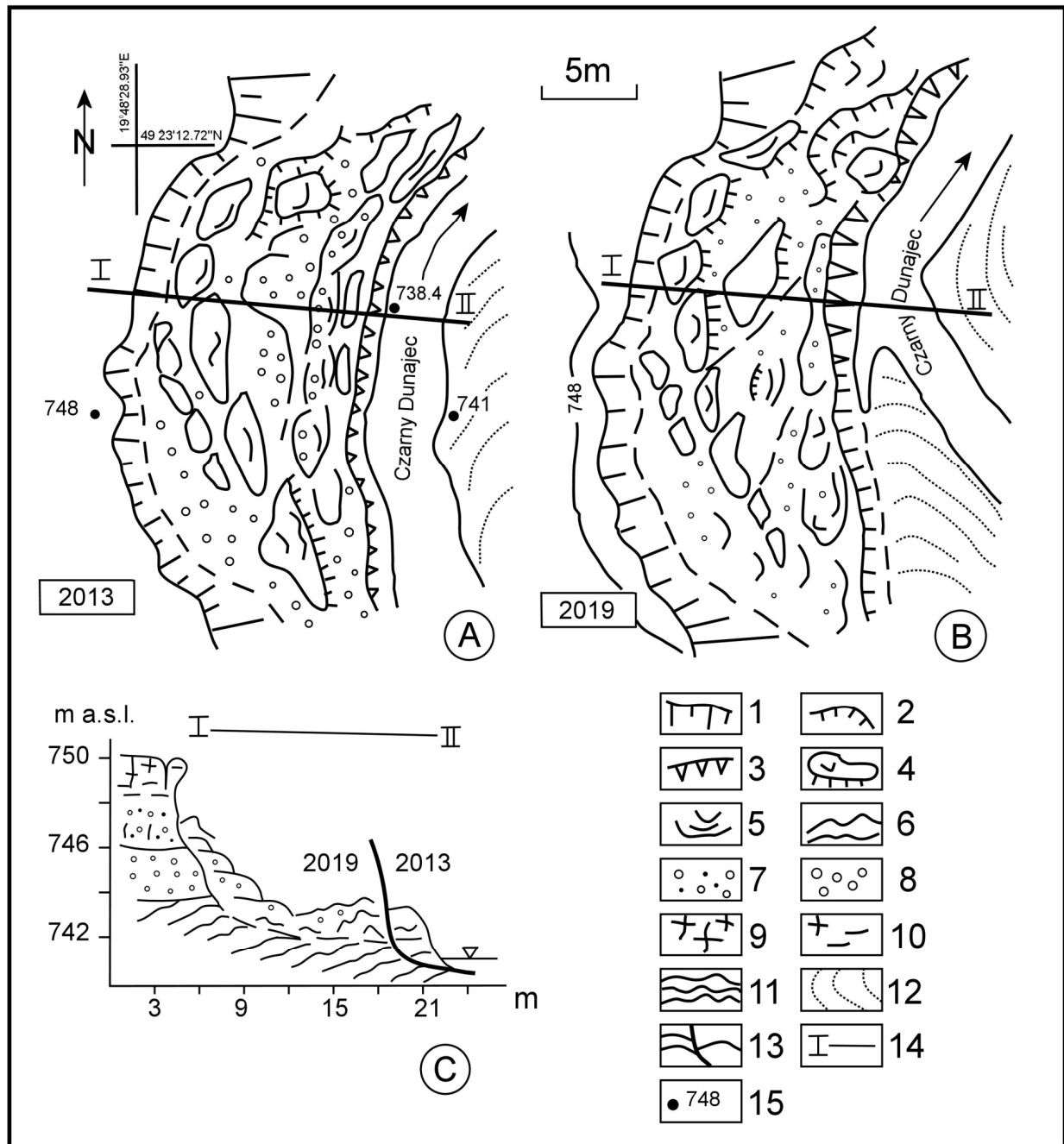


**Figure 7.** Transformation of the C-RCZ at site 1 in years 2013–2019; (A)—2013 r.; (B)—plan of the landslide and river channel in 2019 r.; (C)—cross-section through the landslide and the C-RCZ; 1—main scarp of the landslide, 2—stable scarps on the landslide tongue, 3—last recorded position of the eroded front of the landslide tongue, 4—slices of colluvium, 5—ridges of gravel–clay colluvium, 6—displaced mudstones, 7—alluvium composed of clays and gravels, 8—alluvial gravels, 9—silt deposits, 10—mud deposits, 11—Neogene mudstones and claystones, 12—gravel–sand bars, 13—surface of fluvial erosion in the period 2013–2019, 14—cross-section line I–II, 15—m a.s.l.

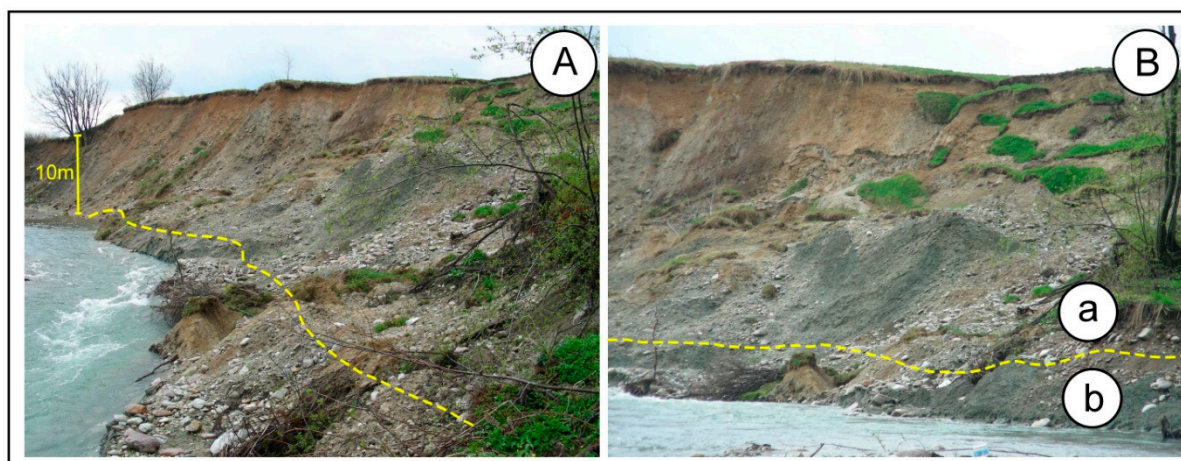


**Figure 8.** Colluvium composed of gravel with silt and mudstone with clay (A) overlying the undisturbed foundation (B) of Neogene clayey mudstones in Chochołów (1) landslide; dashed line marks the trace of the detachment surface; (a)—colluvium, (b)—undisturbed (mudstones and claystones) landslides bedrock base.

The greatest annual volume of material during the study period— $26 \text{ m}^3$ —was eroded in 2014. Waters of the risen Czarny Dunajec River have then three times reached the level of 250 mm and remained as high for 4–6 days. The front of colluvium was intensely eroded over the whole its length of 50 m that year. Large loss of colluvium and its mudstone foundation occurred also after two large episodes of high river stage in 2017, when the water levels reached values similar as in 2014. Loss of material was much smaller in 2013, despite the fact that erosion progressed over the whole length of the landslide front. Correspondingly, the water level rises and water level oscillation were smaller during that year. The length of the active C-RCZ decreased markedly in July 2018, as a result of deposition of a gravel bar at the feet of the previously eroded front of colluvium (Figure 7B). The volume of eroded colluvium and its mudstone foundation decreased only slightly because the river channel along the active bank deepened and the supply of colluvium from the advancing landslide front to the north increased. The C-RCZ shifted laterally toward the landslide main scarp by 1.5–2.5 m in the period 2013–2019 (Figure 7C).

At site 2 the volume of colluvium removed in the period 2013–2019 was small— $43 \text{ m}^3$  (Table 2). Erosion affected the landslide front unevenly. Along the E–W trending section of the C-RCZ (Figure 9A,B), lateral erosion removed both gravel-and-clay colluvium and massive Neogene mudstones from its low-rising foundation. The front of colluvium is there elevated by more than 3 m above the normal river level and the water did not reach it during the high river stages (Figure 9B). In this section, the loss of colluvium was small—20–25% of the total.

Potentially, this section is predisposed to faster fluvial erosion, as colluvium in this part of the landslide is most saturated with water leaking from the adjacent peat bog. The long-lasting inflow of acidic waters not only accelerates weathering of the crystalline clasts in the gravel in the escarpment and in colluvium, turning them into granular clay, but also makes them more susceptible to creeping into the river bed when wet. However, in a straight section of the channel, the river flows around the colluvium, eroding it only slightly.

Erosion was more effective (75–80% of the total material removed from this site) at the bend of the C-RCZ and over its S–N trending section. Mainly colluvium was eroded there, while the mudstone foundation largely remained unaffected. The front of colluvium is there low, 0.7–1.5 m, and is frequently flooded during elevated river stages (Figure 9C). Colluvium was then washed out to the channel and the mudstones remained as a rocky floor.

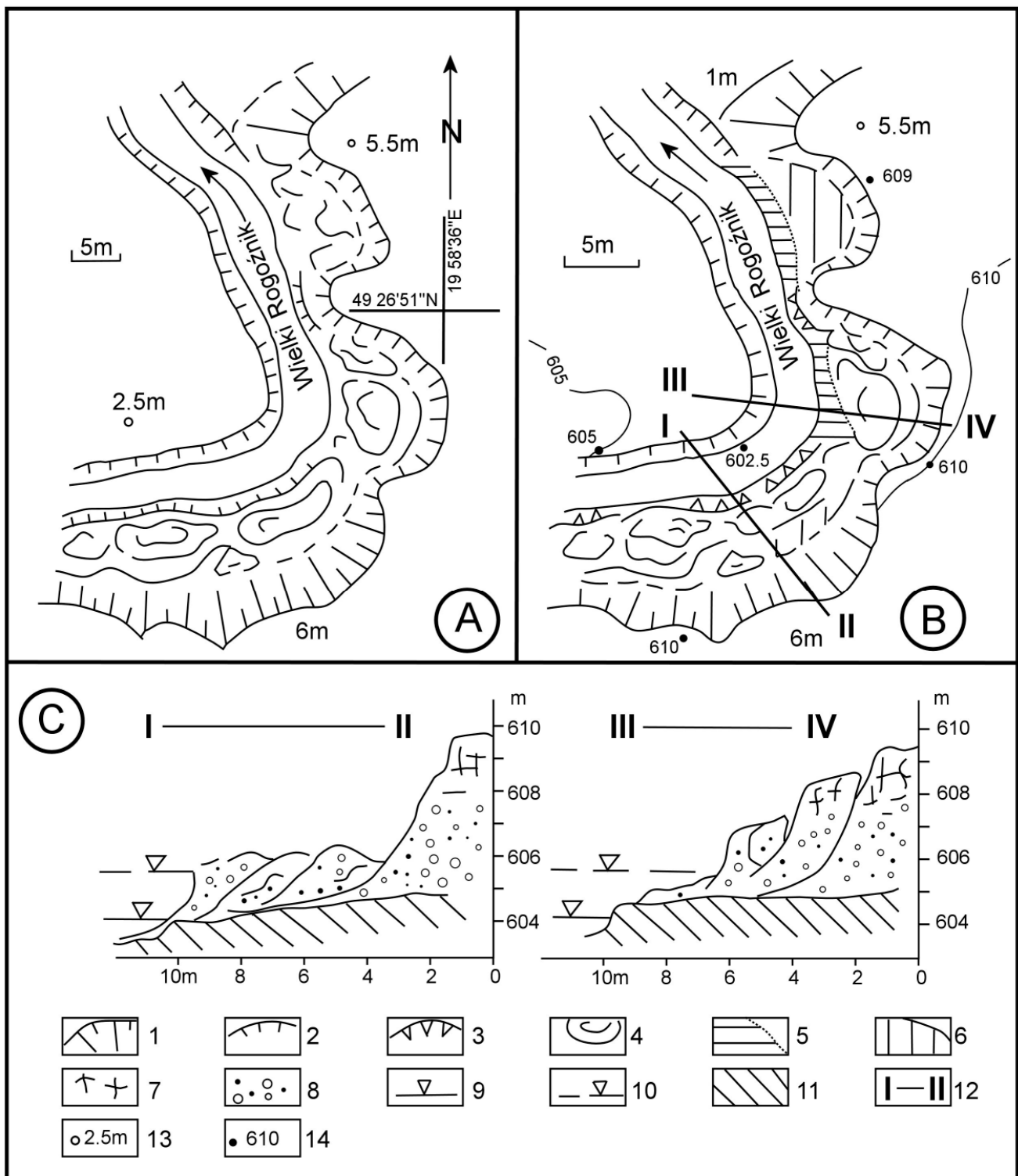


**Figure 9.** Transformation of the C-RCZ at site 2 in years 2013–2019; (A)—plan of the landslide and river channel in 2019; (B)—various modes of the C-RCZ modification and their location; (C)—cross-sections through the landslide and its C-RCZ; 1—landslide main scarp, 2—stable undercutting at the channel bank, 3—erosional undercutting of colluvium, 4—colluvial ridges, 5—part of colluvium flooded during high river stages, 6—surface of the landslide undergoing rejuvenation, 7—silt cover on the 6–7 m terrace, 8—weathered crystalline gravel, 9—mean river stage, 10—high river stage, 11—Neogene claystones and mudstones, 12—cross-section lines, 13—relative height, 14—m a.s.l.

The volume of colluvium eroded at this site was greatest, 7–9 m<sup>3</sup>, in the same years as at site 1. Especially large losses of colluvium have been noted in May 2014 and in 2018 after violent rises in river stage, up to the warning level—280 cm. In the period 2013–2019 the locus of the greatest erosion was migrating along the C-RCZ in pace with changing curvature of the river channel bend.

At site 3 the volume of colluvium eroded during the period of study totaled ca. 140 m<sup>3</sup>. The temporal distribution of this value corresponded to the size and frequency of high river stages each year, and first of all to successive phases of mass movement on the expanding landslide. The C-RCZ is 48 m long and consists of three sections, each having colluvium deposited at different time (Figure 10A). Section I in the northern part corresponds to an episode from 2014. It is 25 m long and it initially consisted of two slices of colluvium, separated by fissures and composed of mudstones interlayered with sandstones and of mudstones interlayered with claystones. The slice marked *a* in Figure 10A, less displaced from the main scarp, was higher (3 m), its internal structure was less deformed and it invaded the river channel to the distance of 1 m only. The front of the other slice, marked *b* in Figure 10A, was 1–2 m high above the current river bed, its layers were strongly inclined and it pushed more than 2.5 m into the river, forcing the flow toward the opposite bank. The landslide was partitioned into slices rotating independently of one another as a result of displacement directed obliquely to the attitude of strata, and of various colluvium displacement.

The second section of this C-RCZ was 23 m long in 2018 and it consisted of colluvium that entered the river channel in 2018 (II in Figure 10A). Most of the colluvium fell directly into the channel. This mass of colluvium consisted of blocks of cohesive claystones, mudstones, and sandstones, and of finer material coming from the mostly sandy sediments present near the top of the bank. The mass of colluvium laid down at base of slope was 1.3–1.7 m high and it shifted the channel margin by 1.5–2.5 m away from the landslide. The upper and southern lateral segments of this landslide were reactivated in 2019 (Figure 10B). The detachment lies at a greater depth in the part of the landslide situated higher on slope, closer to the landslide crown, and built of friable sandstones. The detachment is shallower lower on the slope, in the part of the landslide built of firmer mudstones and claystones. The front of blocky colluvium in the river channel in this part of the landslide was 10 m long, up to 1.2 m high, and up to 1.3 m wide. This was the third (III in Figure 10A), youngest section of the C-RCZ. The first section, dating from 2014 was 25 m long, the second—from 2018—13 m, a the third—from 2019—10 m.

As the individual sections of the landslide front differ in age of colluvium, the durations of erosion and redeposition of colluvium by the river during the period 2013–2019 also differed between the sections: from 5.5 years at section I to 5 months at section III. Till November 2019, 45 m<sup>3</sup> of colluvium was removed from section I, 40 m<sup>3</sup> from section II, and 15 m<sup>3</sup> from section III. The length of the landslide tongue intrusion into the river channel at section I was reduced by half and its height decreased by compaction and downward creep (Figure 11A). At section II all colluvium was removed downstream and the river has eroded also ca. 12 m<sup>3</sup> from the bank surface (Figure 11B). As much as 18 m<sup>3</sup> was eroded at section III. The locus of maximum erosion was migrating upstream.

The migration of the locus of maximum erosion was forced by transformations in channel geometry during successive high river stages, the most important being the increasing angle of attack of the main flow on the bank (Figures 10B and 12A), from initially oblique to perpendicular at the third section (Figure 12B).

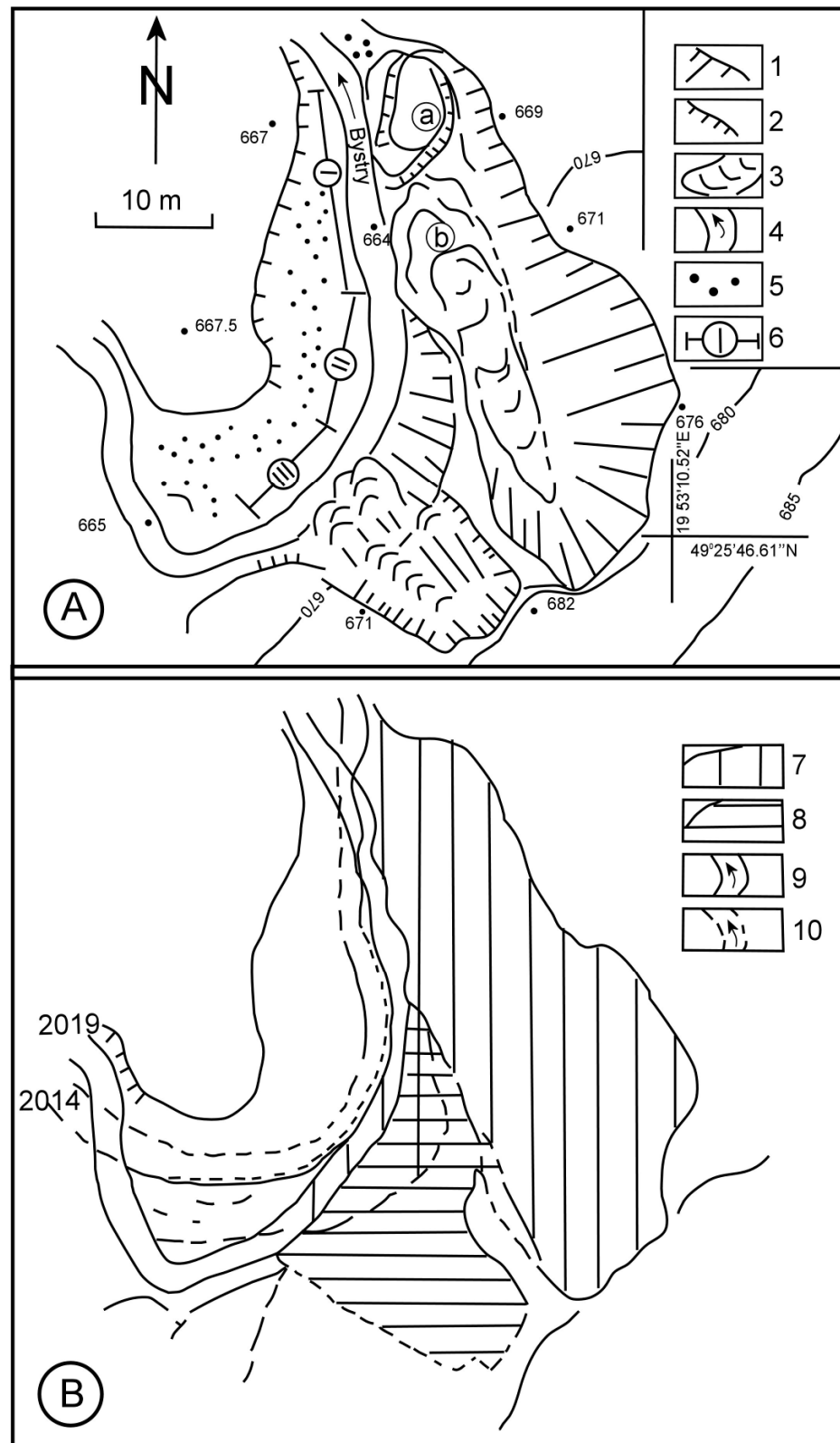


**Figure 10.** Transformation of the C-R CZ at site 3 in years 2013–2019; (A)—plan of the landslide and river channel in 2019; (B)—stages of landslide reactivation: 1—landslide main scarp, 2—erosional undercutting of the channel bank, 3—colluvial tongue, 4—river channel, 5—lateral gravel bar, 6—sections of the C-R CZ; 7—landslide surface in 2013, 8—surface of landslide rejuvenation in 2019, 9—position of the main flow in 2019, 10—position of the main flow in 2013.

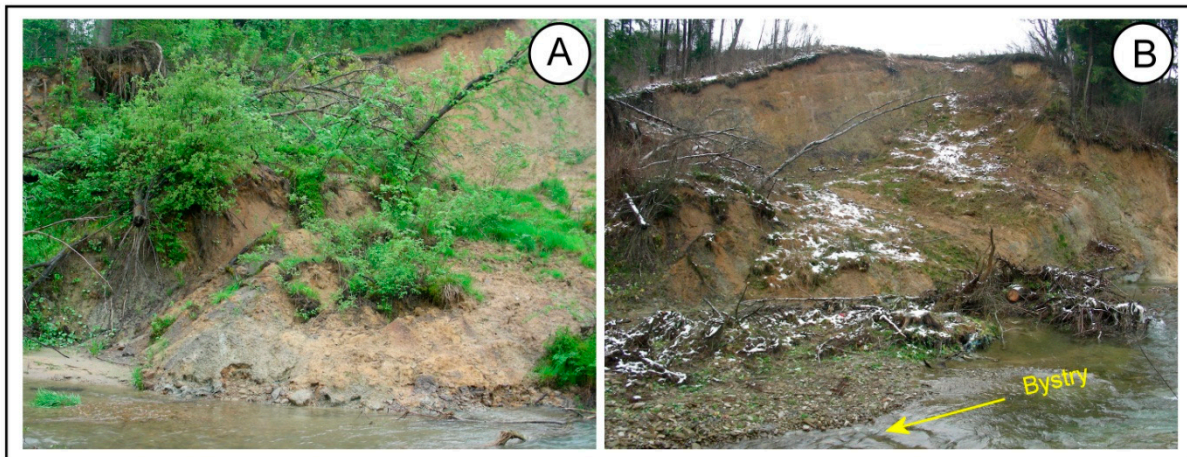


**Figure 11.** Erosion of colluvium by the Bystry River (3) after water level rises in 2014 (A) and in 2018 (B).

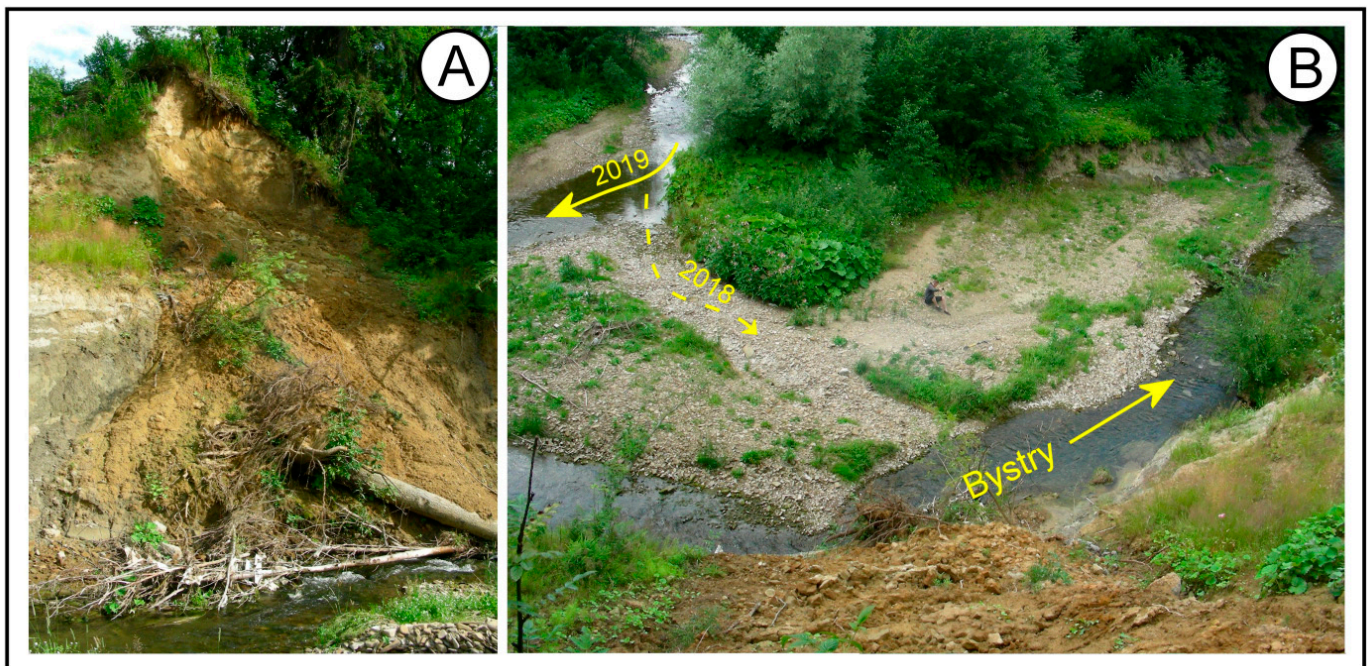


**Figure 12.** Rejuvenation of the landslide at section III (A) and rearrangement of the main flow of the river in 2019 (B) (site 3).

Site 4 (Figure 13A,B) features the lowest volume of eroded alluvium—4–8 m<sup>3</sup>. The front of the piled-up landslide tongue was being eroded slowly. Coarse-grained colluvium that had slid to the channel in cohesive slices hampered the processes of fluvial erosion, even during high river stages. Erosion of the landslide front and removal of the eroded material away from the C-RCZ was selective, depending on the grain-size of colluvium and its cohesion. Three sections differing in the type and intensity of channel processes could be distinguished over the length of the C-RCZ. Over the initial section the Cichy River laterally eroded the colluvial ridge and brought gravelly deposits from the upstream part of its course. In the middle section, the channel was constricted and it went around the huge, up to 10 m thick, landslide tongue composed of an unbroken slice of flysch rocks slid far into the channel (Figure 14A). Weathering and mass-wasting was prevailing on the landslide toe resulted in supply large solid boulders and finer rubbles to its feet. Debris of shales was being readily taken away during each high river stage. The channel bottom at

the downstream end of the C-RCZ was armored with great sandstone blocks originating from the landslide front. Groundwater seeping through the landslide tongue toward the channel favored creep of colluvium and formation of steep scarps at the channel bank. Erosion of the ridge was affected also by water drained from the landslide surface, which dissected the ridge and supplied rubble along with an admixture of clay to the Cichy River channel. The river did not remove the biggest blocks away from the C-RCZ, hence they armor the channel bottom (Figure 14B). As this C-RCZ lies in the upper course of the Cichy River, discharges and river stages here are lower than at the other sites.

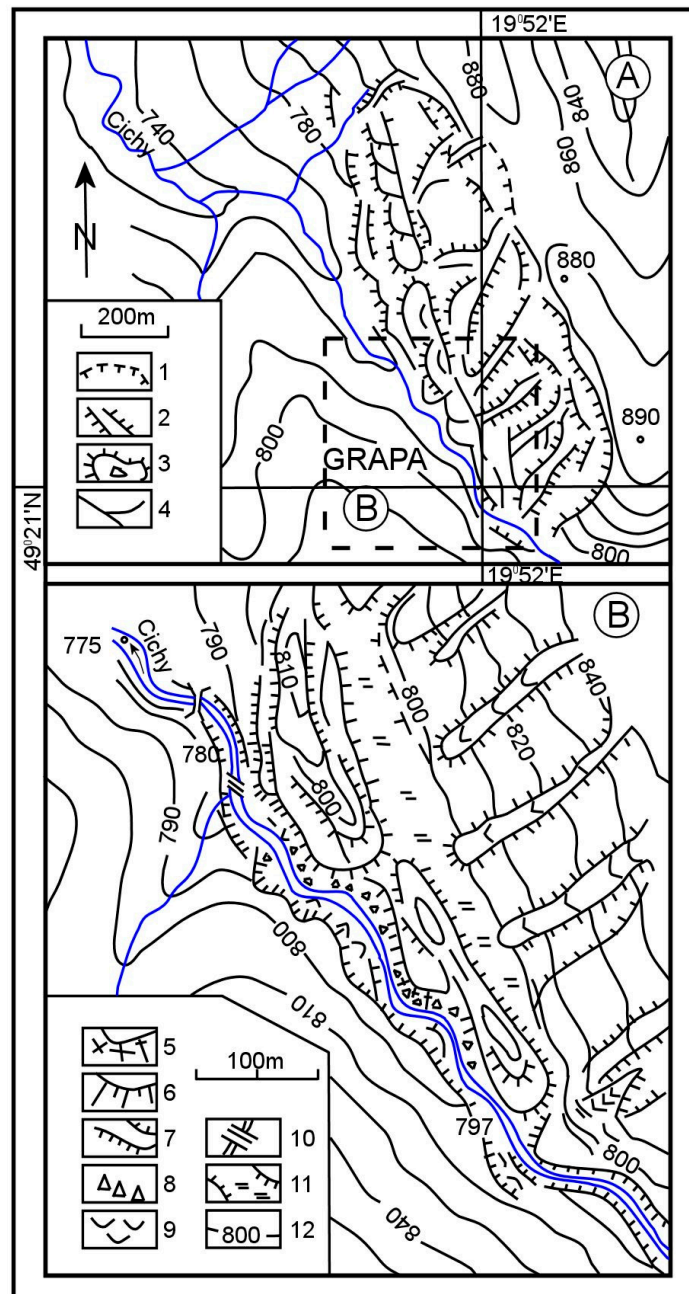


**Figure 13.** Grapa landslide on the slope of the Cichy River valley (A) and its C-RCZ—site 4 (B): 1—main scarp of the landslide, 2—elongated colluvial ridges, 3—colluvial ridges, 4—river channels, 5—rock cliffs, 6—erosional scarps higher than 5 m, 7—edges of colluvial ridges and erosional scarps up to 5 m high, 8—rock debris, 9—single rock falls, 10—rocky steps in the river channel, 11—wet trench on the landslide, 12—elevation contours.

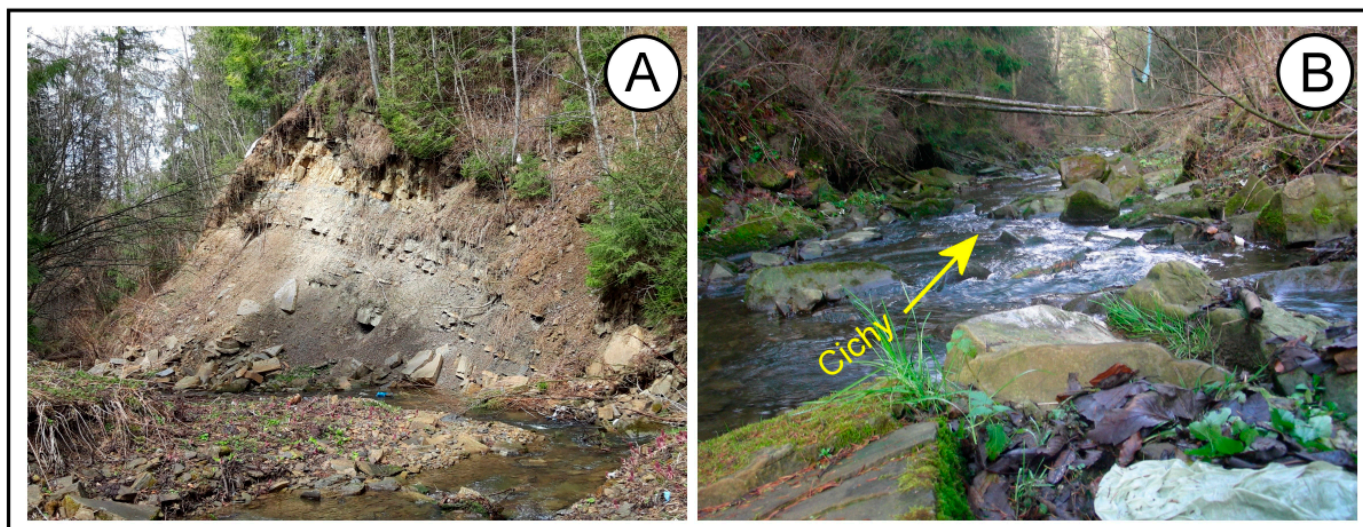


**Figure 14.** A slice of flysch rocks at the front of the Grapa landslide (A) and the channel of the Cichy River armored with the sandstone blocks eroded from the landslide front (B).

#### 4.3. The Amount and Course of Colluvium Erosion in 2019

This was a year of relatively low river stages in the Podhale region (Figure 2), but with large and frequent changes in water levels. Given that, our measurements were carried out most times (six) that year. The volume of colluvium eroded at the studied sites was one of the highest in the 7 years studied, and erosion of colluvium at all C-RCZs was intensified during high river stages. The relation between the volumes of colluvium removed and river stages for hydrological year 2019 is presented in detail in Table 3.

**Table 3.** Volumes of colluvium eroded from the studied landslides in 2019.

Site	Volume of Colluvium Removed from the Landslide Fronts (m <sup>3</sup> )						Total
	20.01–9.02	22.02–12.03	29.04–22.05	19.06	11–15.08	09–10.09	
Chochółów (1)	1.5	2	3.5	3	4	1.5	15.5
Ludźmierz (2)	1	2	2	0.5	1.5	0.5	7.5
Czerwona Góra (3)	2.5	3.5	5	3	5.5	3.5	23
Grapa (4)	1	1.5	1.5	0.5	1	0.5	6
Total (1 + 4)	6	9	12	7	12	6	52

The values of colluvium loss were coincident with the timing of high river stages, and with prolonged duration of the high river stages as well (Figure 15). The loss of colluvium from a stable landslide at site 1 during the elevated river stage on the Czarny Dunajec River, lasting from the end of February through the third decade of May 2019, was comparable to the loss after the greatest, short-lasting high river stage in August of the same year (Table 3). A similar situation was observed at site 3, though there a supply of new colluvium from the active landslide to the river channel could play a role.

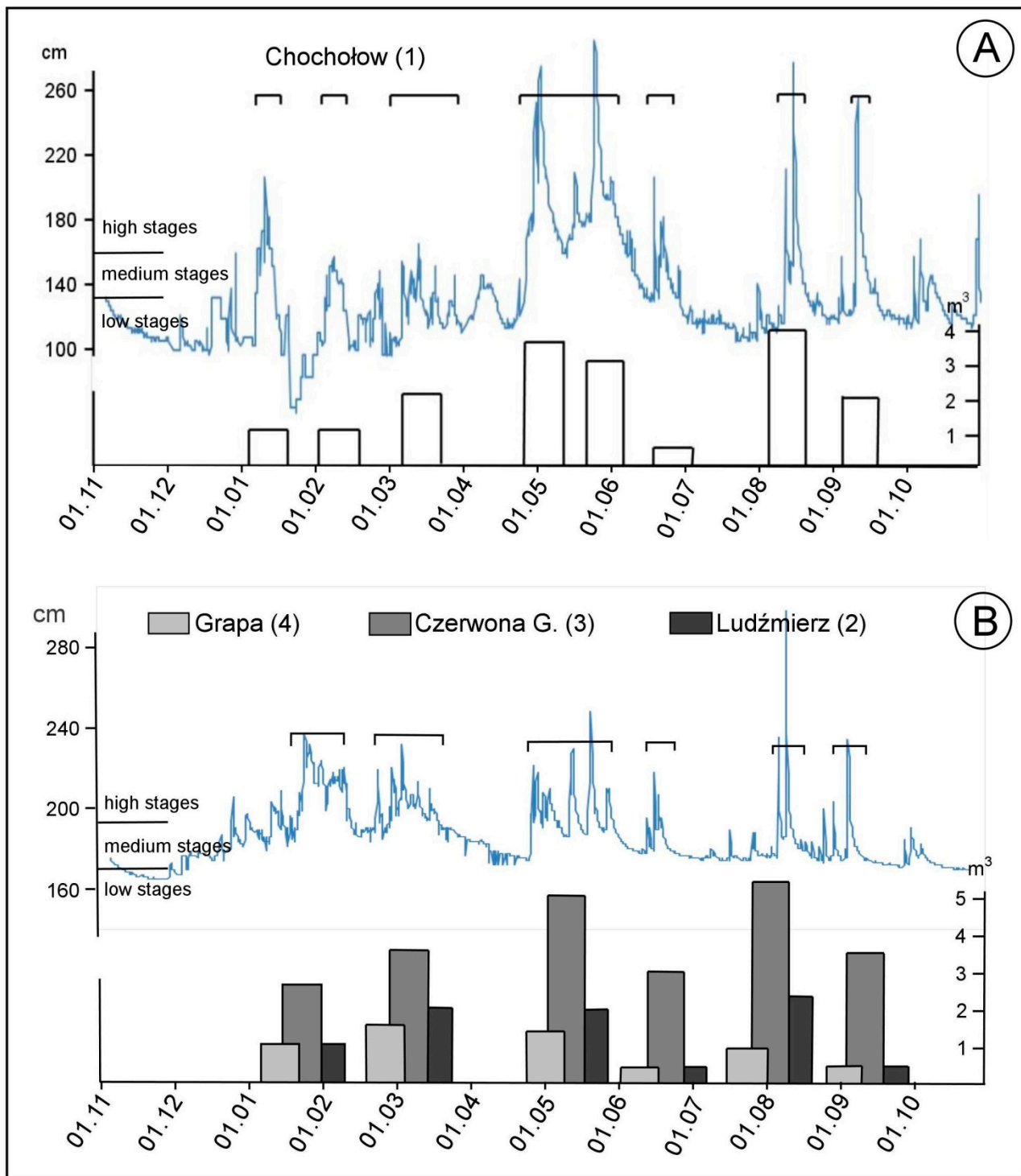


**Figure 15.** Relations between volumes of eroded colluvium (columns) and water levels (curve) on the Czarny Dunajec (A) and Wielki Rogoźnik (B) rivers in 2019; the interval of high water levels is marked with horizontal line and brackets mark the distinguished phases of colluvium erosion.

**5. Discussion**

Local differences in the course and effects of erosion between the C-RCZs may be largely attributed to the hydrodynamic regimes of the rivers. Fluvial erosion of colluvium in all sites was intensified during every rise in river stage above the average. Our sites are situated in mountain rivers where processes of erosion, transport, and deposition of sediments are assumed to be active only at discharge values higher than average, in contrast

to the lowland rivers [62]. The same is valid for erosion of non-colluvial banks of other rivers [63–67].

The periods of prolonged high river stages were those ones of active erosion. Comparison of the volumes of colluvium removed at each site with the duration of erosion shows that erosion was active mainly during prolonged high rivers stages, which means it was related to the water level and discharge. Timing and duration of active erosion and water levels between the Czarny Dunajec (site 1) and Wielki Rogoźnik (sites 2, 3 and 4) rivers is not simultaneous, which is explained by the different nature of their drainage basins. The high river stages on the Czarny Dunajec River were mostly caused by increased precipitation or thaws in the Tatra Mountains, later or longer than in the foothills. Both catchments differ in amounts and timing of precipitations as well as in timing and duration of thaws. For example, in 2019 the Wielki Rogoźnik River experienced high river stage 6 times while the Czarny Dunajec River 7 times. The former one had only one episode of high river stage in 2014 but the effects in erosion at sites 2, 3 and 4 were much higher than at site 1. The spring rises in river stage resulted in greater loss of colluvium by fluvial erosion in the Wielki Rogoźnik watershed (sites 2, 3 and 4) than on the Czarny Dunajec River (Figure 15).

The observed differences in the measurable effects of fluvial erosion in the C-RCZs may be also explained by the differences in physico-mechanical properties of colluvium, especially cohesion, grain-size composition, and texture. Sediments being involved in a landslide have reduced cohesion relative to their initial state [68,69]. The least cohesive is colluvium composed of Quaternary massive gravel at sites 1 and 2. Its resistance to flowing water is reduced by high porosity cf. [69]. Clays roofing the gravels, and fine sands and silts intercalated with gravels, are more cohesive and more resistant to fluvial erosion. Friable colluvium composed of gravel and clay at site 1 was easily washed out from its argillaceous foundation and transported away from the landslide area. Increased resistance of the strath under gravelly deposits to fluvial erosion was related to its massiveness and low absorptivity [70]. The strath at site 1 was eroded at a lower rate by falling down to irregular blocks. The retreat of the landslide front due to erosion stimulated farther supply of colluvium to the erosional escarpments at the front (Figure 16). The volume of colluvium removed by fluvial erosion increased after successive episodes of high river stage.

The much lower volume of eroded colluvium, similar in its cohesion to landslide 1, at site 2 may be explained by the relevant height of its frontal ridge and stabilization of its surface by perennial vegetation. Half of the ridge upstream was not overflowed during the highest stages of the river; on the other hand, the ridge itself prevented supply of colluvium from the upper part of the landslide. Colluvium was then mostly eroded in the eastern half of the C-RCZ length, subject to flooding, where the ridge completely washed away. The more cohesive and firm colluvium composed of mudstone and sandstone which easily disintegrates upon sliding at site 3 was subject to creep and settling. Only the argillaceous intercalations among them are massive, firmer, and display greater resistance to shearing [71]. Its erosion by the Bystry River was slower, but more effective. It proceeded by soaking and softening, decomposition to loose grains, and washing away from the landslide area. The large volume of colluvium eroded from the front of this landslide was largely due to supply of fresh colluvium as a result of two events of the landslide reactivation. Additionally, the large power of the river approaching the landslide front at a right angle favored effective erosion. Among the lithological varieties of colluvium present in the C-RCZs, slices of Oligocene flysch and rubble with an admixture of clay remain the most cohesive at site 4. Their erosion by water is selective. Low efficiency of fluvial erosion at this site was mainly due to that nature of alluvium, and to low power of the low-discharge river confronted with the channel bottom and the feet of the landslide front armored with large sandstone blocks. Armoring of the bottom and the banks was crucial for availability of colluvium to fluvial processes [14,72,73]. Limited surface exposed to erosion, hampered erosion efficiency, and forced grain-size selection of eroded material all contributed to the very slow progress of colluvium removal at this site.



**Figure 16.** Erosion of the mudstones and claystones that underlie colluvium at site 1.

The volume and location of the increased erosion of colluvium in all C-RCZs were also dependent on the spatial patterns of the individual zones. Erosion was most efficient and rapid on concave bends of the channels and in places where the rivers approached the landslide fronts at a high angle, as at sites 1, 2 and 3. While erosion on the concave bends is distributed over a long section of the river bank, erosional power of a river approaching a landslide front at a high angle is focused on a small fragment of the bank and is the most effective (site 3, Figures 10B and 12B). The places where a river attacks the front of colluvium at a high angle and is forced to a sharp change in direction of flow are marked by a niche in the bank and by a short distance to the place of redeposition of the eroded material. The large power of the river approaching the landslide front at site 3 was obviously responsible for the large volume of eroded colluvium, the undercutting of the bank, and the downfall of another fragment of the river bank to the channel (sections II and III on Figure 10). At arcuate bends, the eroded material is redeposited farther away (site 1). Similar patterns have been found earlier for fluvial erosion of river banks and valley slopes [2,35,74].

Besides the factors related to hydrodynamics and morphology of the rivers, the course and scale of colluvium removal from the C-RCZs also directly or indirectly depended on other factors. The high river stages were directly caused by abundant rainfall or sudden thaws. High river stages lasting for many days forced rises of phreatic level in colluvium adjacent to the channel, inevitably lowering its cohesion cf. [75]. A loss of strength in colluvium could also result from increase in pore pressure during a rapid fall of a flood wave [30]. A similar effect was observed in the infiltrational rise in groundwater level within landslides after a rainfall; this could lead to reactivation of the landslides and thus increase the supply of colluvium to the channels [35,76,77]. During winter seasons processes caused by multigelation contributed to colluvium supply to the river channels: downfall and creeping of rock fragments loosened by thawing of the surface layers of colluvium. This was especially evident on the colluvial slices at site 4. The front of the landslide tongue composed of fractured sandstone and shale layers retreated along the river bank mainly by the action of gravity falling and frost-related processes rather than by fluvial erosion. The material fallen by gravity as a result of these processes within the C-RCZ was not being removed instantaneously, but rather selectively during high river

stages. The role of the river consisted in removing transportable debris away from the foot of the C-RCZ than its erosion. The contribution of the processes triggered by multigelation at site 4 was best marked in January and February 2019. The river stage rose 21 times above the average at that time. Cycles of gelation occurred three times and they caused grain-size sorting of the colluvium surface layer and its later creep down to the channel. The loss of colluvium in all the C-RCZs in the Wielki Rogoźnik River watershed (sites 2, 3 and 4) amounted to nearly one third of the annual value (Table 3). At the same time, thaws in the Tatra Mountains (part of the Czarny Dunajec River watershed) were small and the rises in river stage did not cause as significant erosion of the colluvium at site 1. Because of delayed and prolonged thaw in the Tatra Mountains the curve of the water level in the river was rather smooth (Figure 4). Summer floods were much more effective in erosion and removal of colluvium at this site.

## 6. Conclusions

Our results of the 7-year-long monitoring of the progress in erosion of colluvium in the C-RCZs confirmed the thesis presented earlier: erosion of colluvium is intensified during elevated river stages, e.g., refs. [17,30,74,78,79]. Fluvial erosion at the landslide fronts increased when the water level rose above the average values. It attacked those fragments of colluvium which were in contact with the river water and indirectly triggered gravity mass movements beyond its reach. From hydrological point of view, erosion of colluvium seems to be initiated only after a threshold value of river discharge is exceeded [67], but having available only data on water levels in the studied rivers (Figure 2) we cannot establish the threshold values for discharge. The threshold value of water level is different for every site along the Wielki Rogoźnik River, despite their mutual vicinity, because the sites differ in channel geometry and type of colluvium.

The landslide toes which entered the river channels were eroded by rivers at uneven rates, depending on the size and frequency of high river stages, volumes and texture of colluvium, and spatial pattern of each C-RCZ. Phases of active erosion lasted when river stages remained above average. The greatest losses of colluvium during the study were found during short-lasting (1–2 days) maximum river stages, and also during prolonged (7–10 days) high river stages.

The greatest dynamics of change in the C-RCZs were found at those sites where the volume of colluvium removed by the river was replaced with new supply from reactivated landslides (site 3, partly site 1). Besides the large volume of eroded colluvium these C-RCZs witnessed also modification in geometry of river channels. Transformations of the C-RCZs are slower when the landslide fronts are stable are built of more resistant colluvium, and river channel geometry persists (site 4).

The hydrodynamic factors (size of water-level rises, river dynamics, and fluvial channel geometry) were undoubtedly important regulators of the rate and size of erosion of colluvium intruded into river channels, but not the only ones. Other factors that need to be taken into account are susceptibility of the colluvium to fluvial erosion and contribution from other denudation processes acting seasonally, such as abundant rainfalls or multigelation. The role of these processes in the evolution of the C-RCZs was only mentioned in this paper since it seems to be of minor importance.

Our long lasting investigations enable us to forecast farther evolution of the zones. Recognition of the course and rate of these changes in locally different settings of the river–landslide systems provides base for evaluation of the hazard presented by reactivation of the landslides and potential modifications in geometry of river channels in the landscape where the dense pattern of human activities meets the dynamic element of mountain rivers.

**Author Contributions:** Conceptualization, J.K. and K.A.; methodology, J.K., K.A. and J.O.; software, J.K. and K.A.; formal analysis, J.K. and J.O.; investigation, J.K. and K.A.; resources, J.K., K.A. and J.O.; data curation, J.K. and K.A.; writing—original draft preparation, J.K.; writing—review and editing, J.K. and J.O.; visualization, J.K., K.A. and J.O.; supervision, J.K. and J.O.; project administration, J.K.; funding acquisition, J.K. and K.A. All authors have read and agreed to the published version of the manuscript.

**Funding:** The study was financed as a Statutory Project of Pedagogical University of Cracow.

**Institutional Review Board Statement:** Not applicable.

**Informed Consent Statement:** Not applicable.

**Data Availability Statement:** MDPI Research Data Policies.

**Conflicts of Interest:** The authors declare no conflict of interest.

## References

- Ohmori, H. Dynamics and erosion rate of the river running on a thick deposit supplied by a large landslide. *Z. Geomorphol. Suppl.* **1992**, *36*, 129–140. [[CrossRef](#)]
- Owczarek, P. *Transformacja Koryt Rzecznych w Warunkach Dostawy Grubofrakcyjnego Materiału Stokowego (na Przykładzie Średniogórskich Dopływów Odry i Wisły)*; Wydawnictwo Uniwersytetu Śląskiego: Katowice, Poland, 2007; Volume 2510, pp. 1–133.
- Owczarek, P. Hillslope deposits in gravel-bed rivers and their effects on the evolution of alluvial channel forms: A case study from the Sudetes and Carpathian Mountains. *Geomorphology* **2008**, *98*, 111–125. [[CrossRef](#)]
- Strużyński, A.; Kulesza, K.; Strutyński, M. Bed Stability as a Parameter Describing the Hydromorphological Balance of a Mountain River. In *Experimental and Computational Solutions of Hydraulic Problems*; GeoPlanet: Earth and Planetary Sciences; Rowinski, P., Ed.; Springer: Berlin/Heidelberg, Germany, 2013; pp. 249–251.
- Dziuban, J. Osuwisko Połoma. *Czas. Geogr.* **1983**, *54*, 369–376.
- Costa, J.E.; Schuster, R.L. Documented historical landslide dams from around the world. *U.S. Geol. Surv. Open File Rep.* **1991**, *91–239*, 1–486.
- Clague, J.J.; Evans, S.G. Formation and Failure of Natural Dams in the Canadian Cordillera. *Bull. Geol. Surv. Can.* **1994**, *464*, 1–44.
- Hewitt, K. Catastrophic landslides and their effects on the Upper Indus streams, Karakoram Himalaya, northern Pakistan. *Geomorphology* **1998**, *26*, 47–80. [[CrossRef](#)]
- Casagli, N.; Ermini, L. Geomorphic analysis of landslide dams in the Northern Apennine. *Jpn. Geomorphol. Union Trans.* **1999**, *20*, 219–249.
- Haczewski, G.; Kukulak, J. Early Holocene landslide-dammed lake in the Bieszczady mountains (Polish East Carpathians) and its evolution. *Studia Geomorphol. Carpatho-Balc.* **2004**, *17*, 61–85.
- Panek, T.; Smolková, V.; Hradecký, J.; Sedláček, J.; Zernitskaya, V.; Kadlec, J.; Pazdur, A.; Řehánek, T. A Late-Holocene evolution of a floodplain impounded by the Smrdutá landslide, Carpathians Mountains (Czech Republic). *Holocene* **2013**, *23*, 218–229. [[CrossRef](#)]
- Schneider, J.F.; Gruber, F.E.; Mergili, M. Recent cases and geomorphic evidence of landslide-dammed lakes and related hazards in the mountains of Central Asia. In Proceedings of the Second World Landslide Forum, Rome, Italy, 3–9 October 2011; pp. 1–6.
- Griffiths, G.A.; McSaveney, M.J. Sedimentation and river containment on Waitangitona alluvial fan—South Westland, New Zealand. *Z. Geomorphol.* **1986**, *30*, 215–230. [[CrossRef](#)]
- Aipassa, M.I. Landslide Debris Movement and its Effects on Slope and River Channel in Mountainous Watershed. *Res. Bull. Coll. Exp. For.* **1991**, *48*, 375–418.
- Hovius, N.; Stark, C.P.; Allen, P.A. Sediment flux from a mountain belt derived from landslide mapping. *Geology* **1997**, *25*, 231–234. [[CrossRef](#)]
- Oszczypko, N.; Golonka, J.; Zuchiewicz, W. Osuwisko w Lachowicach (Beskidy Zachodnie): Skutki powodzi z 2001 r. *Przegląd Geol.* **2001**, *50*, 893–898.
- Othman, A.; Gloaguen, R. River Courses Affected by Landslides and Implications for Hazard Assessment: A High Resolution Remote Sensing Case Study in NE Iraq–W Iran. *Remote Sens.* **2013**, *5*, 1024–1044. [[CrossRef](#)]
- Korup, O. Landslide-induced river channel avulsions in mountain catchments of southwest New Zealand. *Geomorphology* **2004**, *63*, 57–80. [[CrossRef](#)]
- Korup, O. Geomorphic imprint of landslides on alpine river systems, southwest New Zealand. *Earth Surf. Processes Landf.* **2005**, *30*, 783–800. [[CrossRef](#)]
- Cebulski, J. Human impact on the change of direction of river channel migration caused by formation of a landslide dam. *Studia Geomorphol. Carpatho-Balc.* **2016**, *50*, 5–17.
- Sah, M.P.; Mazari, R.K. Anthropogenically accelerated mass movement, Kulu Valley, Himachal Pradesh, India. *Geomorphology* **1998**, *26*, 123–138. [[CrossRef](#)]

22. Paul, S.K.; Bartarya, S.K.; Rautela, P.; Mahajan, A.K. Catastrophic mass movement of 1998 monsoons at Malpa in Kali Valley, Kumaun Himalaya, India. *Geomorphology* **2000**, *35*, 169–180. [[CrossRef](#)]
23. Lévy, S.; Jaboyedoff, M.; Locat, J.; Demers, D. Erosion and channel change as factors of landslides and valley formation in Champlain Sea Clays: The Chacoura River, Quebec, Canada. *Geomorphology* **2012**, *145–146*, 12–18. [[CrossRef](#)]
24. Dauksza, L.; Kotarba, A. An analysis of the influence of fluvial erosion in the development of a landslides slope (using the application of the queueing theory). *Studia Geomorphol. Carpatho-Balc.* **1973**, *7*, 91–104.
25. Alexandrowicz, S.W. Subfosylna malakofauna z osuwiska w Piwnicznej (Polskie Karpaty Fliszowe). *Folia Quat.* **1985**, *56*, 79–99.
26. Margielewski, W. Landslide forms on Połoma Mountain in the Sine Wiry Nature Reserve, West Bieszczady. *Ochr. Przyr.* **1991**, *49*, 23–29.
27. Margielewski, W. Wpływ ruchów masowych na współczesną ewolucję rzeźby Karpat fliszowych. W. In *Współczesne Przemiany Rzeźby Polski*; Starkel, L., Kotarba, A., Kostrzewski, A., Krzemień, K., Eds.; Instytut Geografii i Gospodarki Przestrzennej UJ.: Kraków, Poland, 2008; pp. 69–80.
28. Cebulski, J. Współoddziaływanie osuwisk i koryt rzecznych w polskich Karpatach fliszowych. Ph.D. Thesis, Polska Akademia Nauk, Kraków, Poland, 2021.
29. Cebulski, J. Impact of river erosion on variances in colluvial movement and type for landslides in the Polish Outer Carpathians. *Catena* **2022**, *217*, 106415. [[CrossRef](#)]
30. Tyszkowski, S. Badania rozwoju osuwisk w rejonie Świecia, na podstawie materiałów fotogrametrycznych. *Landf. Anal.* **2008**, *9*, 385–389.
31. Banach, M.; Kaczmarek, H.; Tyszkowski, S. Rozwój osuwiska w strefie brzegowej sztucznych zbiorników wodnych na przykładzie osuwiska centralnego w Dobrzyniu nad Wisłą, zbiornik wrocławski. *Przegląd Geogr.* **2013**, *85*, 397–415. [[CrossRef](#)]
32. Teisseyre, H. Materiały do znajomości osuwisk w niektórych okolicach Karpat i Podkarpacia. *Rocz. PTG* **1936**, *12*, 133–192.
33. Gil, E. Monitoring ruchów osuwiskowych. In *Zintegrowany Monitoring Środowiska Przyrodniczego; Monitoring Geoekosystemów Górskich*; Szymbark, Poland, 1995; pp. 120–130.
34. Bober, L.; Thiel, K.; Zabuski, L. Zjawiska osuwiskowe w polskich Karpatach Fliszowych. In *Geologiczno-Inżynierskie Właściwości Wybranych Osuwisk*; Wydawnictwo IBW PAN: Gdańsk, Poland, 1997; pp. 1–102.
35. Zydroń, T.; Gruchot, A. Wpływ opadu deszczu i erozji bocznej na stateczność na przykładzie osuwiska w Bieśniku (Beskid Niski). *Acta Sci. Pol. Archit.* **2016**, *15*, 149–161.
36. Williams, D.R.; Romeril, P.M.; Mitchell, R.J. Riverbank erosion and recession in the Ottawa area. *Can. Geotech. J.* **1979**, *16*, 641–650. [[CrossRef](#)]
37. Fletcher, L.; Hungr, O.; Evans, S.G. Contrasting failure behaviour of two large landslides in clay and silt. *Can. Geotech. J.* **2002**, *39*, 46–62. [[CrossRef](#)]
38. Ouimet, W.B.; Whipple, K.X.; Royden, L.H.; Sun, Z.; Chen, Z. The influence of large landslides on river incision in a transient landscape: Eastern margin of the Tibetan Plateau (Sichuan, China). *GSA Bull.* **2007**, *119*, 1462–1476. [[CrossRef](#)]
39. Boengiu, S.; Simulescu, D.; Oana, I.; Popescu, L. River undercutting and induced landslide hazard. The Jiu River valley (Romania) as case study. *Geomorphol. Slovaca Bohem.* **2011**, *2*, 46–58.
40. Cui, P.; Dang, C.; Zhuang, J.Q.; You, Y.; Chen, X.Q.; Scott, K.M. Landslide-dammed lake at Tangjiashan, Sichuan province, China (triggered by the Wenchuan Earthquake, May 12, 2008): Risk assessment, mitigation strategy, and lessons learned. *Environ. Earth Sci.* **2012**, *65*, 1055–1065. [[CrossRef](#)]
41. Wen, B.P.; Aydin, A.; Duzgoren-Aydin, N.S.; Li, Y.R.; Chen, H.Y.; Xiao, S.D. Residual strength of slip zones of large landslides in the Three Gorges area, China. *Eng. Geol.* **2007**, *93*, 82–98. [[CrossRef](#)]
42. Zyndroń, T. Ocena właściwości wytrzymałościowych gruntów z wykorzystaniem analizy wstecznej na przykładzie jednego z osuwisk na zboczu Wiatrówki (Beskid Niski). *Acta Sci. Pol. Form. Circumiectus* **2016**, *15*, 139–150.
43. Staromłyńska, K.; Zydroń, T. Badania wytrzymałości resztkowej gruntów spoistych z terenów osuwiskowych okolic Szymbarku k. Gorlic. *Acta Sci. Pol. Form. Circumiectus* **2017**, *16*, 173–185. [[CrossRef](#)]
44. Zhang, Y.; Guo, C.; Yang, Z.; Shen, Y.; Wu, R.; Ren, S. Study on shear strength of deep-seated sliding zone soil of zhouchangping landslide in Maoxian, Sichuan. *J. Eng. Geol.* **2021**, *29*, 764–776.
45. Kukulak, J.; Augustowski, K. Landslides on river banks in the western part of Podhale (Central Carpathians). *Geol. Q.* **2016**, *60*, 561–571. [[CrossRef](#)]
46. Cebulak, E. Wpływ sytuacji synoptycznej na maksymalne opady dobowe w dorzeczu górnej Wisły. *Folia Geogr. Ser. Geogr. Phys.* **1992**, *22*, 82–95.
47. Niedźwiedz, T.; Obrębska-Starkłowa, B. Klimat. In *Dorzecze Górnej Wisły. Vol 1*; Dynowska, I., Maciejowski, M., Eds.; Państwowe Wydawnictwo Naukowe: Warszawa, Kraków, 1991; pp. 68–84.
48. Obrębska-Starkłowa, B.; Hess, M.; Olecki, Z.; Trepińska, J.; Kowanetz, L. Klimat. In *Karpaty Polskie*; Warszzyńska, J., Ed.; Wyd. UJ: Kraków, Poland, 1995; pp. 31–47.
49. Cebulska, M. Wieloletnia zmienność maksymalnych opadów dobowych w Kotlinie Orawsko–Nowotarskiej (1984–2013). *Czas. Inżynierii Lądowej Sr. Archit.* **2015**, *62*, 49–60. [[CrossRef](#)]
50. Hess, M.; Leśniak, B.; Rauczyńska-Olecka, D. Stosunki klimatyczno-bonitacyjne obszaru Podhala. *Zesz. Nauk. UJ Pr. Geogr.* **1984**, *58*, 7–63.

51. Augustowski, K.; Kukulak, J. Rates of Frost erosion in River banks with different particle size (West Carpathians, Poland). *Geogr. Fis. Din. Quat.* **2017**, *40*, 5–17.
52. Punzet, J. Zmienność przepływu wód powierzchniowych Tatr I Podhala. *Probl. Zagospod. Ziem Górskich* **1981**, *22*, 155–169.
53. Niedźwiedź, T. Extreme precipitation events on the northern side of the Tatra Mountains. *Geogr. Pol.* **2003**, *76*, 13–21.
54. Żmudzka, E. Contemporary climate changes in the high mountain part of the Tatras. *Misc. Geogr.* **2011**, *15*, 93–102. [[CrossRef](#)]
55. Dynowska, I. Reżim odpływu rzecznego, plansza 32.3 Odpływ rzeczny. In *Atlas Rzeczpospolitej Polskiej*; IG PZ PAN, PPWK im E. Romera S.A: Warszawa, Poland, 1994.
56. Olszak, J.; Kukulak, J.; Alexanderson, H. Revision of river terrace geochronology in the Orawa-Nowy Targ Depression, south Poland: Insights from OSL dating. *Proc. Geol. Assoc.* **2016**, *127*, 595–605. [[CrossRef](#)]
57. Krzemień, K. Zmienność systemu korytowego Czarnego Dunajca. *Zesz. Nauk. Uniw. Jagiellońskiego Pr. Geogr.* **1981**, *53*, 123–137.
58. Birkenmajer, K. *Przewodnik Geologiczny po Pienińskim Pasie Skalkowym*; Wydawnictwa Geologiczne: Warszawa, Poland, 1979; 236p.
59. Michalik, A. Osuwisko w Cichem na Podhalu. *Rocznik Nauk. Dydak. WSP Krakowie* **1962**, *10*, 49–56.
60. Bartarya, S.K.; Sah, M.P. Landslide induced river bed uplift in the Tal Valley of Garhwal Himalaya, India. *Geomorphology* **1995**, *12*, 109–121. [[CrossRef](#)]
61. Millet, D. River Erosion, Landslides and Slope Development in Göta River. Master's Thesis, Chalmers University of Technology, Göteborg, Sweden, 2011; 91p.
62. Bartnik, W. Hydraulika potoków i rzek górskich z dnem ruchomym—Początek ruchu rumowiska wlezonego. *Zesz. Nauk. Akad. Rol. Krakowie* **1992**, *171*, 122.
63. Ziętara, T. Rola gwałtownych ulew i powodzi w modelowaniu rzeźby Beskidów. *Prace Geogr. Inst. Geogr. PAN* **1968**, *60*, 1–116.
64. Harvey, A.M. The influence of sediment supply on the channel morphology of upland streams: Howgill Fells, Northwest England. *Earth Surf. Processes Landf.* **1991**, *16*, 675–684. [[CrossRef](#)]
65. Harvey, A.M. Coupling between hillslopes and channels in upland fluvial systems: Implications for landscape sensitivity, illustrated from the Howgill Fells, Northwest England. *Catena* **2001**, *42*, 225–250. [[CrossRef](#)]
66. Karmaker, T.; Dutta, S. Erodibility of fine soil from the composite river bank of Brahmaputra in India. *Hydrol. Processes* **2011**, *25*, 104–111. [[CrossRef](#)]
67. Göransson, G.; Hedfors, J.; Ndayikengurukiye, G.; Odén, K. Climate change induced river erosion as a trigger for landslide. In Proceedings of the 17th Nordic Geotechnical Meeting, Reykjavik, Iceland, 25–28 May 2016; Volume 1–2, pp. 1182–1192.
68. Thiel, K.; Zabuski, L. Wytrzymałość na ścinanie masywów skalnych fliszu karpackiego. *Pr. Nauk. Inst. Geotech. Hydrot. PWroc.* **1995**, *36*, 330–336.
69. Kaczyński, R. *Warunki Geologiczno-Inżynierskie na Obszarze Polski*; Państwowy Instytut Geologiczny-Państwowy Instytut Badawczy: Warszawa, Poland, 2017; 398p.
70. Julian, J.P.; Torres, R. Hydraulic erosion of cohesive riverbanks. *Geomorphology* **2006**, *76*, 193–206. [[CrossRef](#)]
71. Demonik, A. (Ed.) *Właściwości Wytrzymałościowe i Odształceniowe skał. Centralne Karpaty Zachodnie. Cz. 5 (14). Objąsnienia i interpretacja*; Wyd. Zakł. Geomechaniki IHiGI UW: Warszawa, Poland, 2012; 77p.
72. Weeb, R.H.; Melis, T.S.; Griffiths, P.G.; Elliott, J.G. Reworking of Aggraded Debris fans. In *The Controlled flood in Grand Canyon*; Geophysical Monograph Series; AGU: Washington, DC, USA, 1999; Volume 110, pp. 37–51.
73. Malet, J.-P.; Maquaire, O.; Locat, J.; Remaitre, A. Assessing debris flow hazard associated with slow moving landslides: Methodology and numerical analyses. *Landslides* **2004**, *1*, 83–90. [[CrossRef](#)]
74. Lawler, D.M.; Grove, J.R.; Couperthwaite, J.S.; Leeks, G.J.L. Downstream change in river bank erosion rates in the Swale-Ouse system, northern England. *Hydrol. Processes* **1995**, *13*, 977–992. [[CrossRef](#)]
75. Kim, Y.S.; Wang, Y.M. Landslide Analysis of River Bank Affected by Water Level Fluctuation I. *J. Korean Geosynth. Soc.* **2010**, *9*, 77–85.
76. Iverson, J.P.; Torres, R. Landslide triggering by rain infiltration. *Water Resour. Res.* **2000**, *36*, 1897–1910. [[CrossRef](#)]
77. Barla, G.; Antolini, F.; Barla, M. Slope stabilization in difficult conditions: The case study of a debris in NW Italian Alps. *Landslides* **2013**, *10*, 343–355. [[CrossRef](#)]
78. Banach, M. Dynamika brzegów dolnej Wisły. *Dok. Geogr.* **1998**, *9*, 92.
79. Henshaw, A.J.; Thorne, C.R.; Clifford, N.J. Identifying Causes and Controls of River Bank Erosion in a British Upland Catchment. *Catena* **2013**, *100*, 107–119. [[CrossRef](#)]